INFN-LNL-245(2016)

Report on the construction and performances of four drift cells of the muon chambers of CMS for aging effects studies at LNL

G. Mocellin

Università degli studi di Padova, Padua, Italy

F. Gonella, F. Gasparini, A. T. Meneguzzo

Università degli studi di Padova & INFN sez. Padova, Via Marzolo 8, Padova, Italy

25/11/2016

Abstract

In order to study the effects of aging of the CMS muon Drift Tube chambers, two modules, bicells, were built with the same materials used in the construction of the CMS Drift Tubes. Each bicell is composed by two cells with the same DT cell shape but reduced length. The performances of the bicells are analyzed and verified to be the same of the DT chambers cells in a cosmic muons telescope and with a ^{109}Cd source. The position resolution is about 300 μm; the detection efficiency and electrons amplification have been measured as a function of wires voltage, showing a plateau of efficiency of 98% starting at 3550 V. The signal amplification has been evaluated 10^4 at 3700 V.

1 Introduction

In 2025, Lhc will be upgraded to HighLuminosity-Lhc reaching a luminosity of $5 \times 10^{34}\ cm^{-2} \cdot s^{-1}$, a factor 5 with respect to the actual luminosity. The rate in the DT chambers of the CMS muon system is expected to increase ~ 10 times the rate the DT chambers were built for.
In fall 2015, one of the spare DT CMS chambers has been used to study the cell behavior under a very large background as would be the case of the HL-Lhc in order to evaluate any aging effects. In these tests, the DT chamber was in the GIF++ [1] and supported an integrated luminosity of the order of 10 times the full foreseen HL-Lhc within a 100 smaller time widow.
In such very stressing test, the performances of the chamber presented a degradation on the efficiency and on the performances (trigger capability) showing aging effects. At a direct (SEM[1)]) inspection of the wires of some cells, a deposition of low Z substances (C, O, Si) was recorded.
In order to be able to perform specific tests on the DT cells (such as for identifying the origin of such deposition or for measuring the rate of the aging as function of the integrated luminosity [2],[3]) it was decided to build a small prototype of DT chamber cells.

In section 2 a description of a DT cell and chamber is presented.
In section 3 the new double cells system (bicells) is described.
In section 4 the construction of the two bicells is shown.
In section 5 the preliminary tests are presented .
In section 6 the performances of the cells are reported.

2 CMS DT

The basic element of the DT system is the drift cell (figure 1). The cell has a transverse size of $42 \times 13\ mm^2$ with a $50\ \mu m$-diameter gold-plated stainless-steel anode wire at the center. The wire operates at a voltage of $+3600$ V (at the Cern atmospheric pressure). The gas mixture ($85\%/15\%$ of Ar$\%$/CO_2) provides good quenching properties and a saturated drift velocity of about $55\ \mu m/ns$. Given the cell size, the maximum drift time is around $385\ ns$. The cell design makes use of 4 electrodes (including 2 cathode strips) to shape the effective drift field: 2 on the side walls of the tube, and 2 above and below the wires on the ground planes between the layers. They operate at $+1800$ V and -1200 V respectively. The FE electronics and the HV connections are placed at opposite side of the wires inside the gas flux. Four staggered layers of parallel cells form a superlayer (SL). A DT chamber consists of 2 SLs that measure the r-phi coordinates with wires parallel to the CMS beam line, and an orthogonal SL that measures the r-z coordinate (being r the nominal radial distance from the beam collision point). The DT chambers are 2.5 m long and their length varies, ranging from $1.9\ m$ to $4.1\ m$ [5],[6].
Charged particles crossing a drift cell in the DTs ionize the gas within the cell: due to the shape of the electric field, the produced primary and secondary electrons in $\sim \pm 2\ mm$ above and below the middle plane drift towards the anode amplification wire. The drift time of the primary electrons is obtained from the value of the beginning of the rising time of the Front End (FE) signal (digitized with a high-performance time-to-digital converter (TDC) [7], after the subtraction of a time pedestal). The time pedestal contains contributions from the latency of the trigger and from the propagation time of the signal within the detector and the data acquisition chain. The hit position, i.e. the distance of the muon track with respect to the anode wire, is reconstructed as:

$$pos_{hit} = t_{drift} \cdot v_{drift} = (t_{TDC} - t_{ped}) \cdot v_{drift} \tag{1}$$

where t_{TDC} is the measured time by the TDC, t_{ped} the time pedestal, and v_{drift} the effective drift velocity, which is assumed to be approximately constant in the cell volume, being the E field = constant = $2.3\ kV/cm$ [8].

[1)] Performed with the Scanning Electron Microscope available at LNL by S. Carturan and V. Maggioni

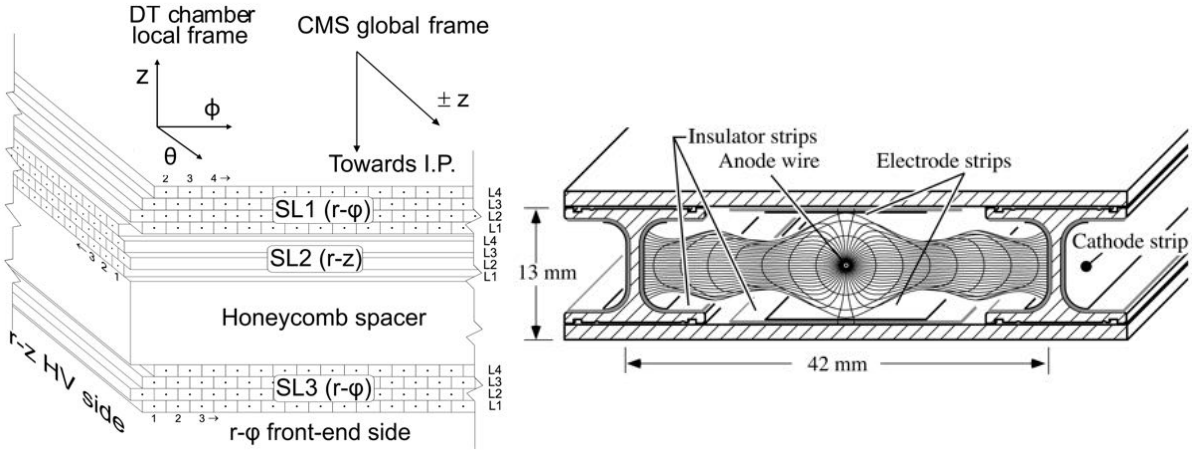

(a) Schematic view of a DT chamber

(b) Section of a drift tube cell showing the drift lines and isochrones

Figure 1: DT chamber and DT cell schematics

3 Design of the two bicells

The bicells are designed as shown in figure 2. They are divided into three different zones: the main central one with the gas active volume, and two smaller ones at its sides, in which all the electronics for high voltage (HV) and signal processing are placed. Such a configuration allows to have the HV and the FE electronics not in contact with the gas fluxing inside the cells.
Aluminium slabs ($1,2m \times 12cm \times 2,5mm$) are used to delimit the entire volume on bottom and top. The top slab is divided into three parts (HV region, FE electronics region and sensitive wire region) which are fixed to the rest of the structure using screws in order to be removable independently. The removable covers allow to inspect the interior of the cells and to change the wires when needed.
The central zone is separated from the two ancillary parts by two aluminium blocks with several holes for gas pipes and for HV cables. These two blocks and the walls of the bicells are glued to the basis as well.
In the active parts the aluminium I-beams ($85cm$ long) are glued to the bottom slab, the gold coated steel anode wires ($50\mu m$ in diameter) will be in the center, and the aluminium strips sticked to the upper and the lower slabs in the middle of each cell. The I-beams are partially covered with Mylar tape for isolating the aluminium strips which serve as cathodes .

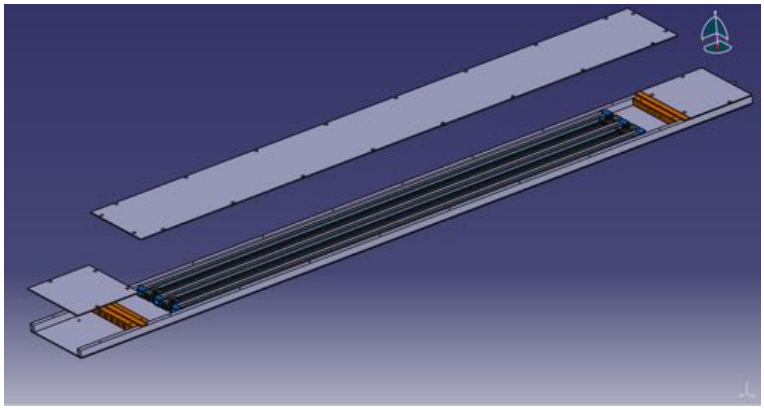

Figure 2: Design of the bicell

The electronic chain for each wire is shown in figure 3. The power supply is connected to a low-pass RC circuit to clean accidental voltage noises and to the anode wire. Between the wire and the electronics of the front end a high-pass RC circuit with a spark gap is placed.
The electronics for the read out is composed by a MAD integrated circuit, with a charge pre-amplificator, a signal shaper, a comparator with a threshold, usually set to a voltage of 20mV, and an output stage [9].

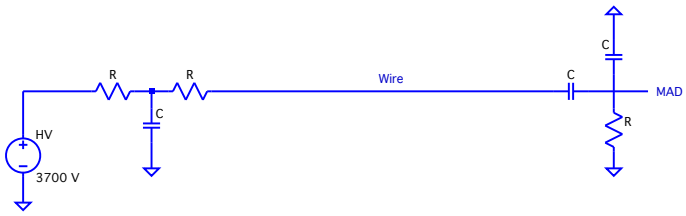

Figure 3: Wire electronical scheme

4 Construction of the two bicells

The two bicells have been assembled in the INFN LNL laboratories in Legnaro (PD, Italy) with spare materials coming from several labs where DT Chambers were built. This detail is of the highest importance because the goal is to reproduce exactly the cells of the DT Chambers, with the same materials and performances, in order to test their aging problems as if they were original DT cells.
While the DT chambers were constructed within a system of high accuracy alignment system ($100\ \mu m$ in positioning the wires), the bicells were entirely hand-made build by some of the technicians and physicists of the INFN sections of Bologna, Padova and Torino who built the CMS DT chambers.
Firstly, the walls and the I-beams (with cathodes pre-attached) were glued to the basis slab using Araldite at a distance of $4,2\ cm$; than electronic cables and copper gas pipes were glued, using DP190, to the blocks which close, in the wire direction, the active region. Swagelok connectors have been used for the gas pipes lines.

(a) Gluing I-beams, wires and gas pipes

(b) Bicell parts description

Figure 4: Construction of the two bicells

After the glue became dry, it was possible to stick with Araldite the blocks to the bottom aluminium slab at an approximate distance of $1\ m$ and to place the anode wires and their plastic supports at the ends of the I-beams.
In the last operation the wires were connected to the electronics and the electronic boards were fixed to the aluminium slab using screws and hex nuts.
Once every component of the cells was in place, the bicells were closed with the three covers using screws and aluminium tape to seal them.

5 Preliminary tests

The first step was to check the gas tightness. After the use of a gas leak tester, in order to identify the leakages, the bicells were dipped in a vessel filled with water. Checking the gas pressure and inspecting the water, issues were found: some in the junction between the aluminium cover and the walls of the cells and some, smaller ones, caused by the electronics cables passthrough. The problems were fixed with more Araldite, aluminium tape and DP190. The final gas tightness of the bicells was checked with a differential barometer: the pressure inside the

cells decreased 1 $mbar$ per hour.
Next step was the checks of the electronics. The bicells have been positioned inside the muon chamber telescope available at LNL. The LNL CMS telescope is composed by two MB3 muon chambers ($237.9cm \times 302.1cm \times 27cm$) as shown in figure 5; the upper chamber is named ch1, the lower one ch2. As reported in [10], in the DT chamber the signals of all channels are hardware analyzed and a "DT Local Trigger segment" signal is output with position, direction and reference time of the crossing ionizing particles (within 25 ns steps). The informations of the ch1 and ch2 and related to the muon events triggered by ch1 (within a window of the track direction), were recorded and analyzed offline [11] for tracks reconstruction. Usual rates for the trigger was 330 $counts/sec$; the rate of each wire of the bicells was instead ~ 6 $counts/sec$, in agreement with their surface ratio.
The output signal of the four wires of the bicells were plugged into four unused channels of the ch1 readout (#0,#9 and #6,#15) and data were registered in the same data files of the chambers wires.
Voltages of cell's electrodes (bicells and chambers) were set as follow: $+3700$ V for anode wires (wire HV setting at the LNL atmospheric pressure), $+1800$ V for strips and -1200 V for cathodes. The pressure inside the cells was set to ~ 10 $mbar$ above atmospheric pressure (~ 1010 $mbar$).
After a preliminary data collection and analysis, comparing the rate of the second hit events of each cell[2)], it was noticed that one cell detected half of the signals. Inspecting the reading electronics and checking the connections between wires and MAD and fixing the spark gap tinning, the problem was solved.

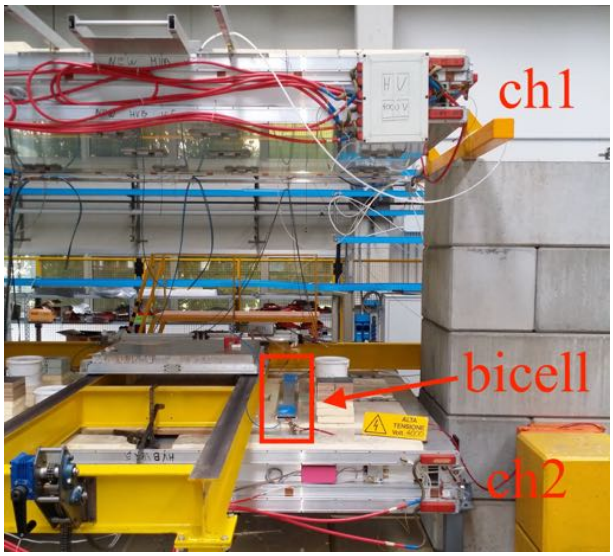

Figure 5: Preliminary tests

6 Tests of the bicells

Once all the hardware was checked to work properly, it was possible to perform the definitive tests. The behavior of a DT cell can be characterized with:

- the distribution of the first hit time (Timebox), whose shape gives informations about the uniformity of the efficiency within the cell and of the electric field shape.
- the linearity of the distribution Time vs Track position, which gives informations about the drift velocity of electrons in gas.
- the resolution of the reconstructed position.
- the detection efficiency as a function of the position of the track in the cell.
- the detection efficiency as a function of the wire voltage (their amplification gain).
- Electrons multiplication around the wire, which gives the signal gain between the ionization electrons created by the cosmic muon in gas and the signal on the wire.

[2)] This method is very sensitive and fast for identifying differences due to gas, electronic cross talk or noise.

6.1 Linearity, resolution, efficiency of the bicells

6.1.1 Experimental setup

Both the bicells were positioned upon ch2 in the MB3 telescope.The wires of ch1 and ch2 are aligned with high accuracy and the two chambers are placed in two parallel planes [12]. In the following we will call ϕ and θ the position measured by the r-phi and r-z SLs of ch2; the z direction is normal to the plane of the ch2 plane (DT chamber local frame, figure 1). The two bicells have been placed with quite a high precision in a plane parallel to the ch2 plane with the wires of the bicells parallel to the $r-\phi$ wires of ch2 and in the same $r-\theta$ position of ch2, in order to simplify data analysis (figure 5). HV was set to $+3700$ V for the wires, $+1800$ V for the strips, -1200 V for the cathodes, which are the same values of the ch1 and ch2 electrodes (standard values at LNL, see [12]); the threshold was set to 20 mV. As in the preliminary tests, the four wire output channels were plugged into four read-out channels (#0,#9,#6,#15).
The following results are based on a data collection run with a total 2 million events (around 2 hours) triggered by ch1. The number of events with just one track well reconstructed either in ch1 or in ch2 are 100K. Considering just geometrical acceptance, the expected good events per cell should be ~ 1800 .

6.2 Data analysis and results

Position of the bicells with respect to ch2

The efficiency of the bicells has been computed using the tracks identified in the ch2 chamber extrapolated to the bicells plane. The distance z of this plane from the z=0 plane of the ch2 chamber has been extracted selecting cosmic muon events with recorded TDC data in the channels associated to the two bicells wires. Selected only the ones with an angle less than 0.1 rad in ϕ and θ plane in ch2, the position in ϕ and θ of such tracks in the two chambers is shown in figure 6; the distributions are broader in ch1 than in ch2 because of the slope acceptance and accuracy and the z distance of the two chambers planes ($\sim 2.5\ m$ for ch1 and $\sim 0.15\ m$ for ch2) from the bicell plane. The width of the ϕ distribution of the selected tracks in ch2 corresponds to the width of two near cells (about $8.4\ cm$).

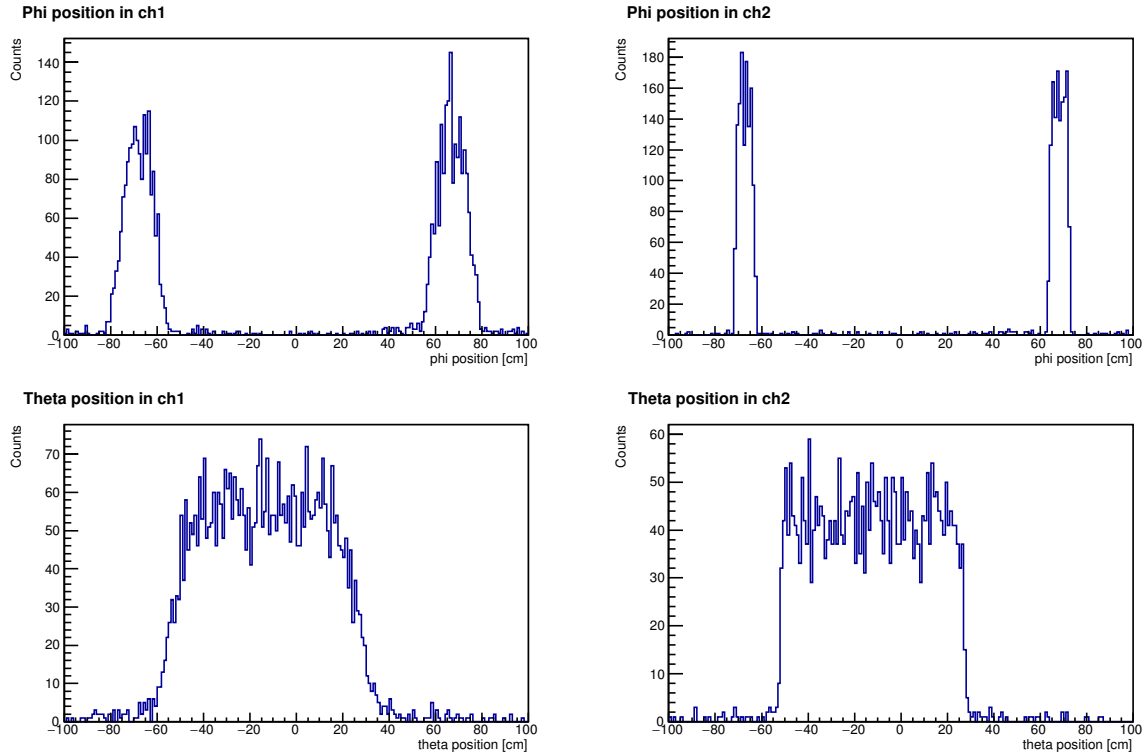

Figure 6: ϕ and θ positions of the bicells: events detected in ch1 and ch2

To find the exact z-position of the bicells plane from the z=0 plane of ch2, given an arbitrary (but reasonable) z of the bicell plane, the extrapolated track position has been considered with respect to the bicells recorded TDC

time[3)]. In figure 7, the distributions relative to different z of the bicells plane are shown. In the plot, for each z position considered, the TDC times have been shifted with common specific delays (values are reported in the legend). The spread of the distributions changes as function of the z of the bicells plane and reaches a minimum around z $= 15.1\ cm$. The ranges of the TDC in the different positions show the drift time range; the "V" shape reflects the symmetry of the TDC time in the left and right position of the cell with respect to the wire. An accurate quantitative evaluation of the z of bicell plane has been obtained with a minimization process of the residuals of the extrapolated position at a given z plane with respect to the the linear fit in each branch of the 'W' distributions.

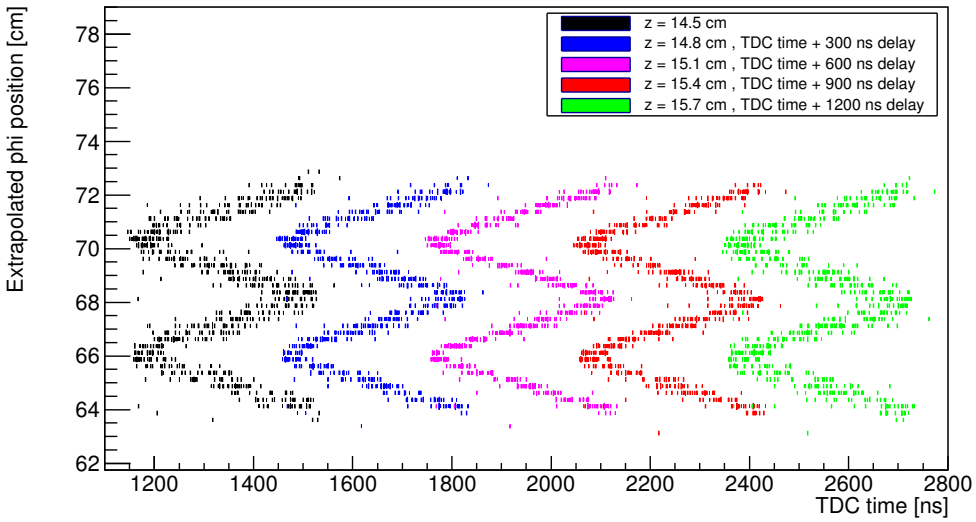

Figure 7: ϕ position of the Ch2 track extrapolated at different z planes vs TDC time: cells #0,#9

	Bicell #0, #9	Bicell #6, #15
Position ϕ [cm]	$64 \div 72.2$	$-71.4 \div -63$
Position θ [cm]	$-52.5 \div 37.5$	$-52.5 \div 37.5$
Position z [cm]	15.1	15.1

Timeboxes

The "timebox" is the distribution of the TDC times recorded by a wire of a bicell or chamber. In figure 8 timeboxes of cell #0, upper plots, and the ones of the ch2 cells, bottom plots, are compared. The bicells and the chambers have the almost same threshold (20 mV for the bicells and 30 mV for the chambers) and the same HV setting (see subsection 6.1.1).
From the "timebox" of the bicell there is almost null noise since no signals are recorded before a starting time and this starting time is almost equal in all the four wire channels. Considering the distribution of the first signal recorded, first hit timebox, the distribution is almost flat in a range of $\sim 400\ ns$ wide. It corresponds to the times of the signal of electrons produced by primary and secondary ionization of cosmic rays in the gas. Due to the fact that cosmic rays are uniformly distributed in space, the first hit timebox is expected to be flat within the full drift time distribution if the effective drift velocity is uniform. The peak after the rising edge of the distribution is due to $\delta-$electrons emitted by the ionizing track; δ-electrons have 50% probability to arrive earlier than the ionization electrons. The rising edge ($\sim 25\ ns$) takes into account of the track time jitter with respect to trigger (ch1 trigger), being the trigger generated with a coincidence of a $40\ MHz$ clock.
Second hit candidate are $\delta-$electrons or electrons extracted from the cell's wall by photons produced in the electron multiplication near the wire. In the timebox $2^{nd} - 1^{st}$, the peak at $\sim 400\ ns$ identifies the photoelectrons extracted from the cathode strips. The FE dead-time of $\sim 60\ ns$ is visible in the "timebox" of the second hit.

[3)] The extrapolated position is calculated as follows: $pos_{extrap} = pos_{ch2} + \phi slope_{ch2} * z$

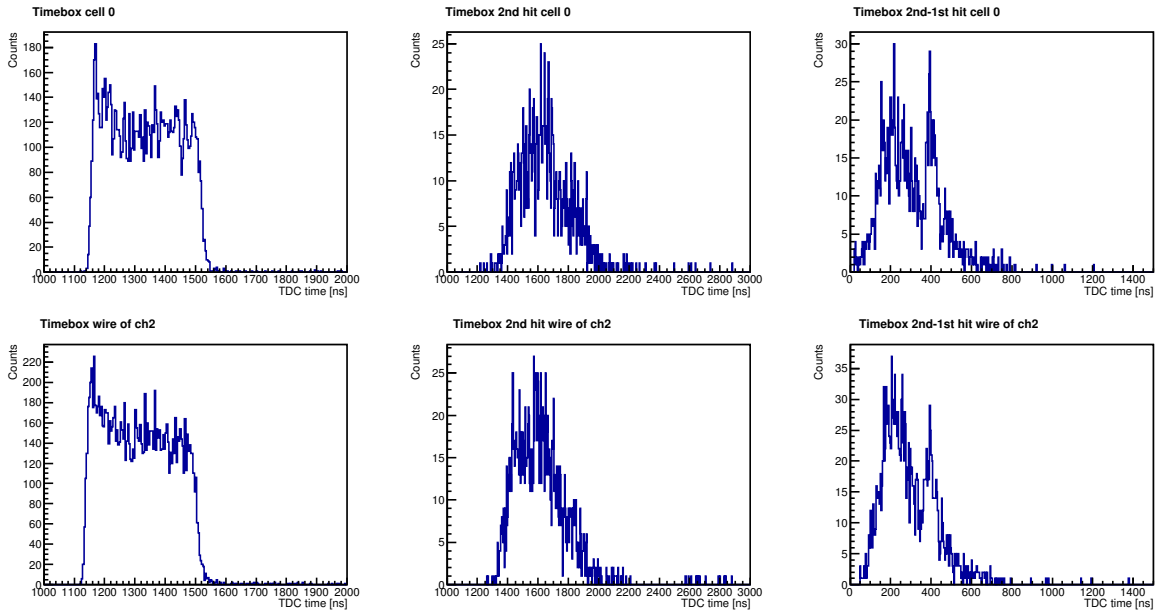

Figure 8: Timeboxes of the cell #0 of the bicells and one of the cell of ch2

Parameters

The parameters for computing the position of the track in the plane of the bicell from the TDC times are the electrons drift velocity in the gas, the ϕ-position of the wires and the TDC offset time (t_{Trig}). The tracks which cross a cell just on the wire position have almost null drift space, then their TDC recorded time is assumed as zero of the TDC time, or t_{Trig}. As can be seen it corresponds to the starting point of the rising of the timebox distribution. These parameters can all be extracted from the distribution of the " Extrapolated position vs TDC time", fitting with a linear regression each branch of the 'W' distribution and considering the weights of each extrapolated position. The absolute value of the slope represents the drift velocity of electrons (v_{drift}), the intersection between two near straight lines (belonging to the same 'V') gives the ϕ-position of the wires (y-axis) and the t_{Trig} (x-axis).
Alternatively, it is possible to obtain the t_{Trig} time from the equation 2, given v_{drift} and $\phi-$position of the wires, plotting it as an histogram and fitting the distribution with a gaussian.

$$t_{Trig} = t_{TDC} + \left| \frac{\phi pos_{extrap} - \phi pos_{wire}}{v_{drift}} \right| \tag{2}$$

The weighted average of the drift velocity is $v_{drift} = 0.0056\ cm/ns$; the results of the parameters ϕ-position of the wires and trigger time obtained are presented in table 1.

	t_{Trig} centroid [ns]	t_{Trig} FWHM [ns]	Wire's $\phi-$ position [cm]
#6 wire	1158.5	25.05	-69.23
#15 wire	1156.7	25.32	-65.03
#0 wire	1150.8.5	24.89	66.03
#9 wire	1150.6	24.73	70.23

Table 1: Parameters of the cells

Linearity in detecting positions of the tracks

To verify the linearity of the position with respect to the recorded drift time in the cells, the distribution 'reconstructed position by ch2 vs detected position by the bicells' has been used. An example is given in figure 9, selecting the cell #15. Detected position is calculated with the equation: $pos_{det} = pos_{wire} \pm (t_{TDC} - t_{Trig})$. The distribution is as expected.

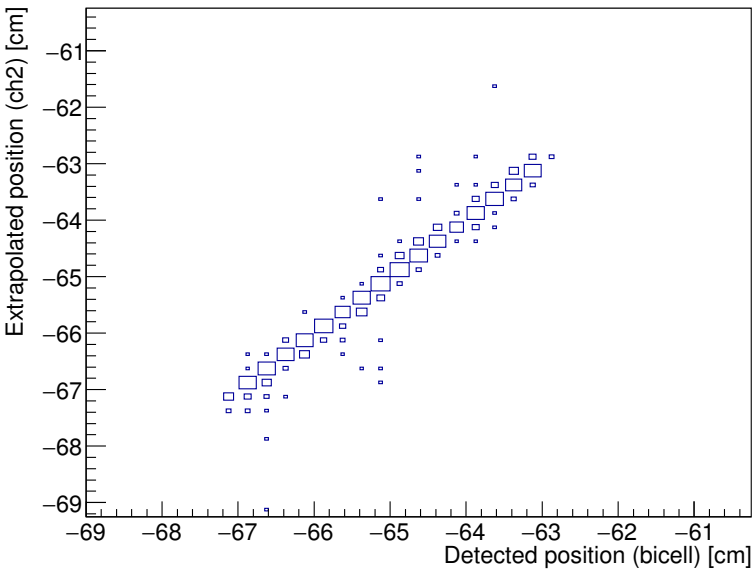

Figure 9: Linearity of the cell $\#15$

Bicells' position detection resolution

Spatial resolution is defined as the σ of the distribution of the difference between the ch2 extrapolated position and the position measured by the bicells(figure 10). Some systematic errors must be taken into account. One is the the track time delay with respect to the trigger time (which defines the start of the TDC): as reported previously the trigger time have a granularity of $25\ ns$, while the cosmic muon tracks have a uniform time distribution. This track delay, event by event is computed within the track reconstruction both in ch1 and in ch2. This track time correction can be applied to the bicells TDC time. Another systematic error is the delay due to the propagation of the signal along the wire. The position along the wire is computed extrapolating the reconstructed θ track in the ch2 and using the propagation velocity of $24\ cm/ns$ as a function of the track's distance from the front-end electronics[5],[4]. Moreover, the obtained new σ is the convolution of the real resolution of the bicells, the error of the reconstructed position in ch2 extrapolated to the plane of the bicells and the one due to multiple scattering, since cosmic muon have low momentum (see equation 3).

$$\sigma^2_{tot} = \sigma^2_{resol} + \sigma^2_{extrap} + \sigma^2_{mult-scatt} \tag{3}$$

Detection efficiency

Detection efficiency is defined as the number of events detected by the bicells related to the number of events passing through the bicells triggered by the chambers (equation 4).

$$Efficiency = \frac{counts_{bicells}}{counts_{chamber}} \tag{4}$$

It is possible to analyze the efficiency of the bicells as a function of the ϕ-position (figures 11,12,13,14) at different voltage. The shape of the efficiency, with respect to the distance of the track from the wire, reflects the electric field shape of the cell (figure 1). Indeed, the primary electrons are uniformly distributed along the track path but only the ones which drift towards the wire will contribute to the avalanche. Where the track cross the cell at a distance from the wire with a short path with lines ending on the wire, there will be a less probability to have enough primary electron to produce a detectable signal at a given HV, i.e. at a given amplification.
The average efficiency as a function of the voltage of the bicells wires is shown in figure 15. These plots show a wide efficiency plateau with a constant value of 98% from 3550 to 3900 Volt. The curves for the four cells are almost identical.

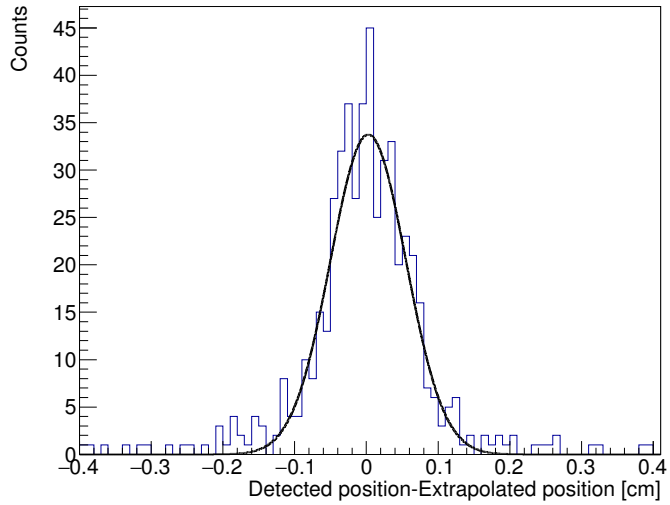

$$\sigma_{tot} = 400\mu m$$

$$\sqrt{\sigma^2_{extrap} + \sigma^2_{multi-scatt}} = 250\mu m$$

$$\sigma_{resol} = 300\mu m$$

Figure 10: Spatial resolution of the bicells, example plot of cell #15

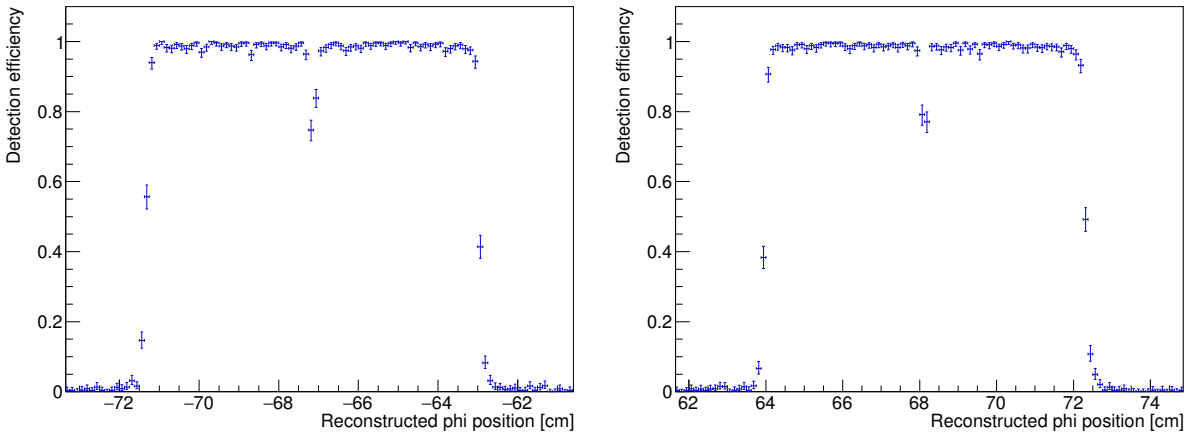

(a) Cells #6,#15

(b) Cells #0,#9

Figure 11: Efficiency of the bicells as a function of the $\phi-$position of the tracks (wire voltage 3700 V)

6.3 Amplification near the wire

One of the visible effect of aging on gas detectors is a lowering of the signal amplification as function of the integrated current. The bicells will be used to studies such effects, thus it is important to evaluate the amplification on the wire to a given release of energy in the cell as in the case of minimum ionizing particle or of gammas from radioactive sources. In these checks of the bicells, the total charge signal produced by a gamma source was measured for evaluating the amplification on the anode wires. These measurements with sources will be easily redone at any time later during aging tests. The important aspect will be the accuracy not on the absolute amplification but the accuracy on the variation of the amplification (before, during and after the aging tests).

6.3.1 Experimental setup

In the upper central cover of the bicells was made a hole (1 mm in diameter) and a collimated radioactive source of ^{109}Cd with an activity of 419 kBq placed above. ^{109}Cd has gamma decays and emits photons with energies of 22 keV (85%) and 24.9 keV (14%) [13]. The gas tightness was maintained covering the hole with Mylar tape (figure 16).
Two different charge preamplifiers with feedback capacitors of 1pF and 7pF were used in order to cover the signals ranges at the different HV setting. The amplified signals were digitized using a 1024-channels MCA.

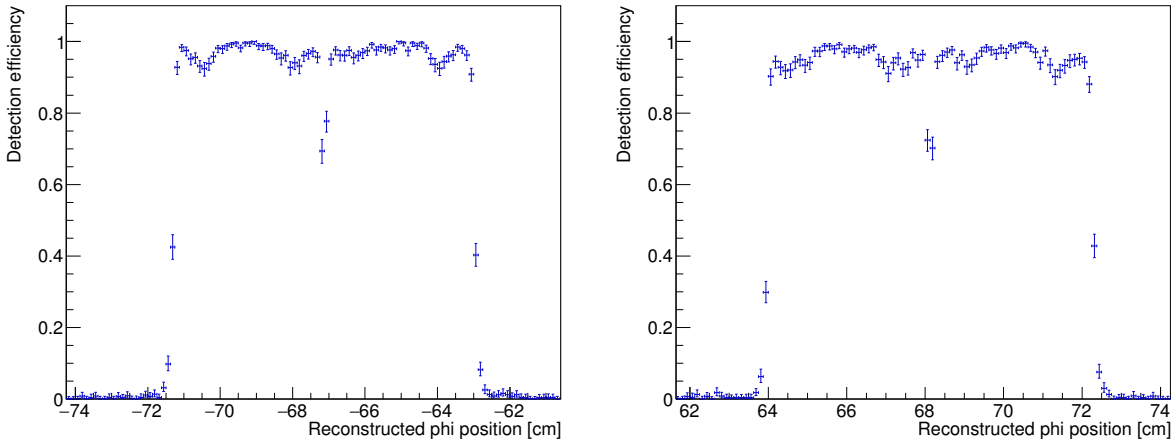

(a) Cells #6,#15 (b) Cells #0,#9

Figure 12: Efficiency of the bicells as a function of the $\phi-$position of the tracks (wire voltage 3550 V)

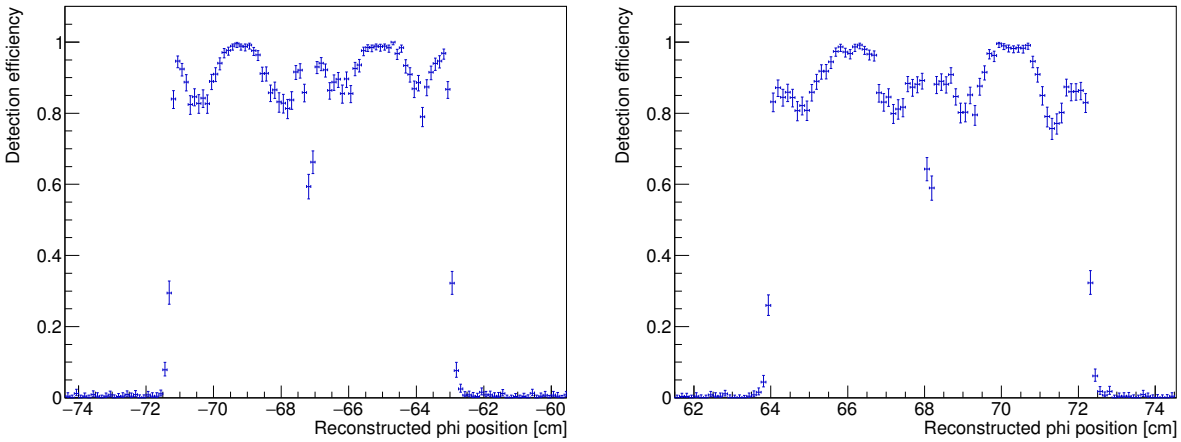

(a) Cells #6,#15 (b) Cells #0,#9

Figure 13: Efficiency of the bicells as a function of the $\phi-$position of the tracks (wire voltage 3500 V)

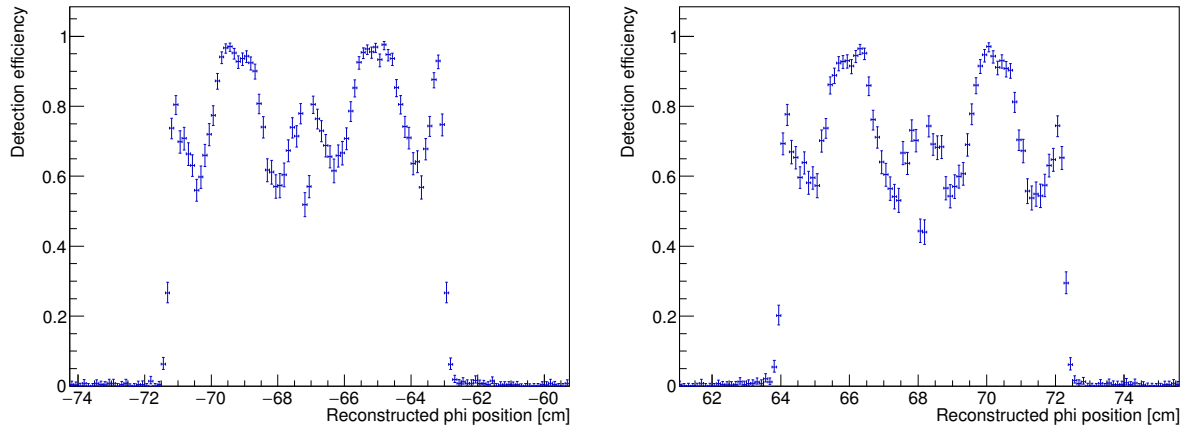

(a) Cells #6,#15 (b) Cells #0,#9

Figure 14: Efficiency of the bicells as a function of the $\phi-$position of the tracks (wire voltage 3450 V)

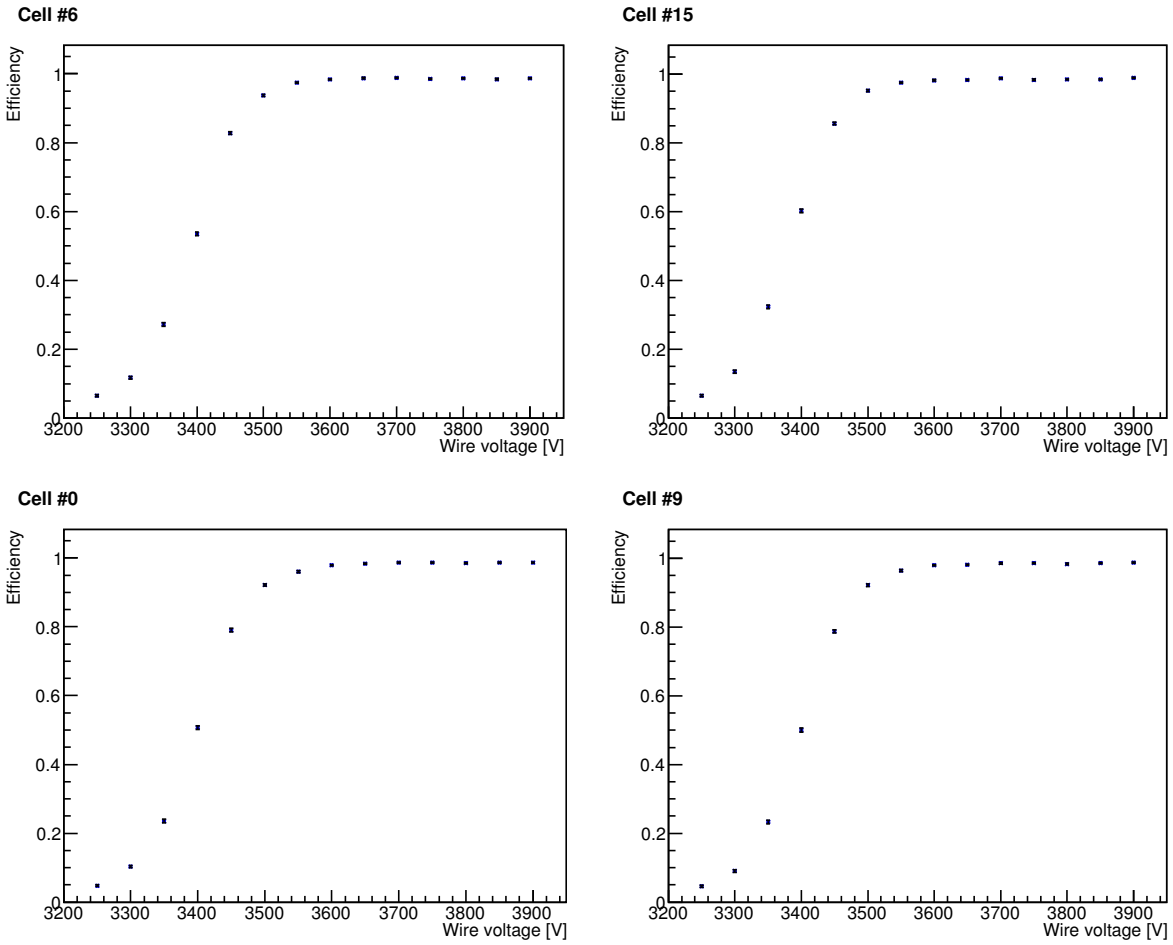

Figure 15: Average efficiency of the four cells as a function of wires HV

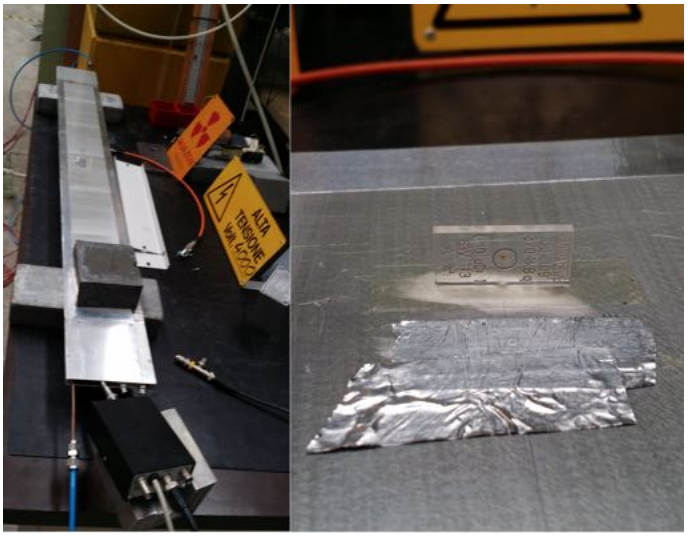

Figure 16: Experimental setup to determine for electrons amplification

6.3.2 Data analysis and results

The weighted average of the energies of the photons emitted by the ^{109}Cd is 22.41 keV. Photons through photo-electric effect (figure 17) gives almost all its entire energy to an electron, which, in Ar/CO_2 gas ($85/15\%$) has a range of $5.7\ mm$ and produces ~ 830 ion-electron pairs ($27.05\ eV$ each). However, the zone of the electric field, inside the cell, from which the electrons produced can drift to the wire, in the specific point of the hole done on the bicell's cover, is $\sim 4\ mm$ wide, thus ~ 580 of the primary and secondary created photoelectrons drift toward the wire producing the amplification and then the detected signal [14].

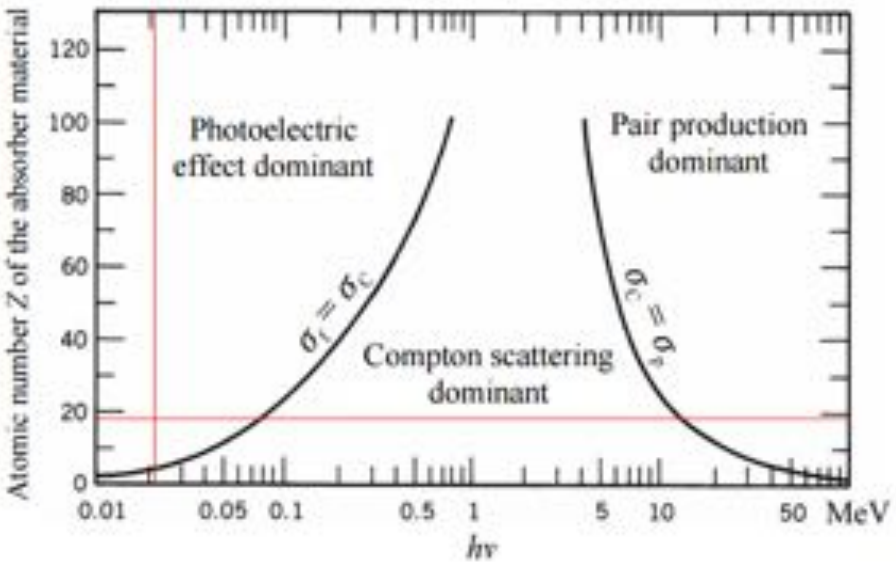

Figure 17: Photons interaction with matter

The signal of the electrons, amplified near the wire, is formed and amplified with 1pF and 7pF pre-amps. After the calibration of the MCA spectra done with known input test voltage signals applied to a 2.2pF test capacitor of the pre-amps (figure 18), the charge spectra are obtained (example in figure 19). The photo-peak distributions, relative to spectra taken varying the wire voltage, are fitted with a LANDAU curve, which center represents the charge collected by the wire. In figure 20 is shown the exponential rising of the amplification, defined as the charge detected by the wire related to the charge of the 580 electrons, as a function of the wires' voltage. Fitting the plot with an exponential curve it is possible to extract the amplification at 3700 V[4)], which corresponds to a value of 1.0×10^5.

The above amplification factor has been computed assuming the zone of the electric field with lines converging to the wire to be constant; in fact, in the DT cell this zone changes as a function of the HV, being thinner at low HV (as could be verified with GARFIELD simulation, but out of the accuracy needed of this test). Assuming the thickness of this zone to be proportional to the efficiency in the whole region (at least above 3450 V, below of which threshold effects would appear), the amplification at 3700 V would be 0.9×10^5.

[4)] It was not possible to have experimental data at HV value of 3700V because of the electronics

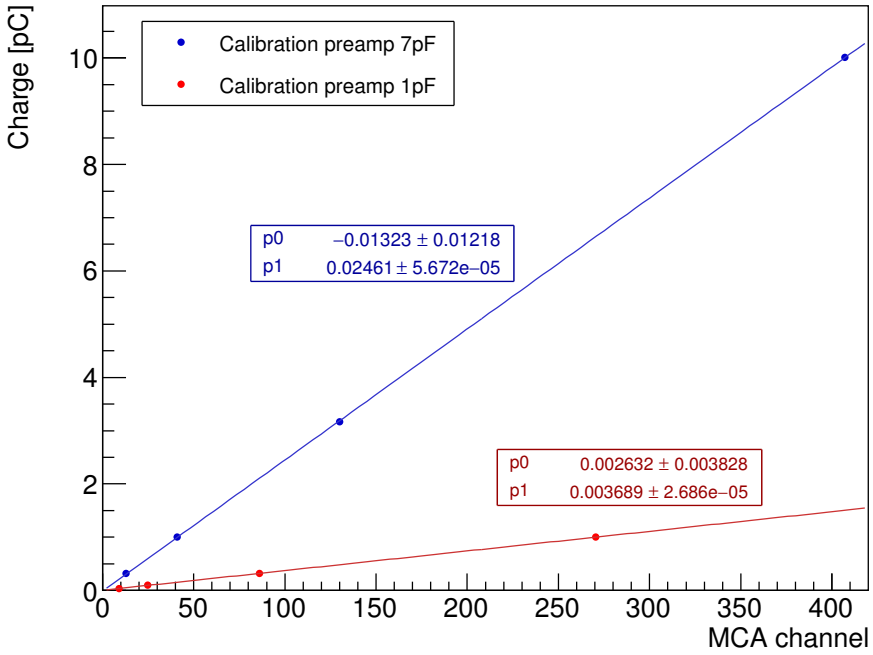

Figure 18: MCA calibration with 1pF and 7pF pre-amps

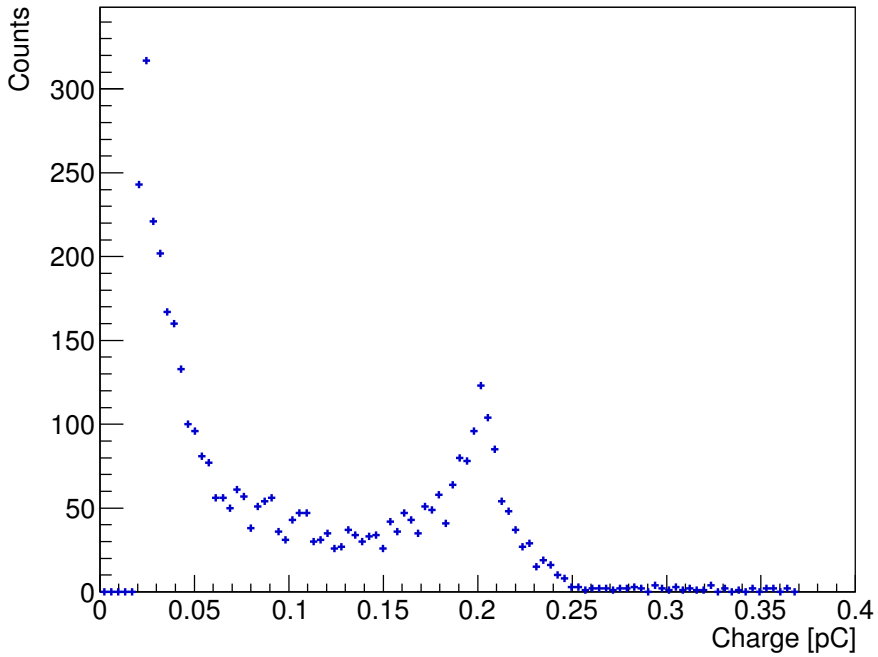

Figure 19: ^{109}Cd charge spectrum, wire voltage set at 3250V

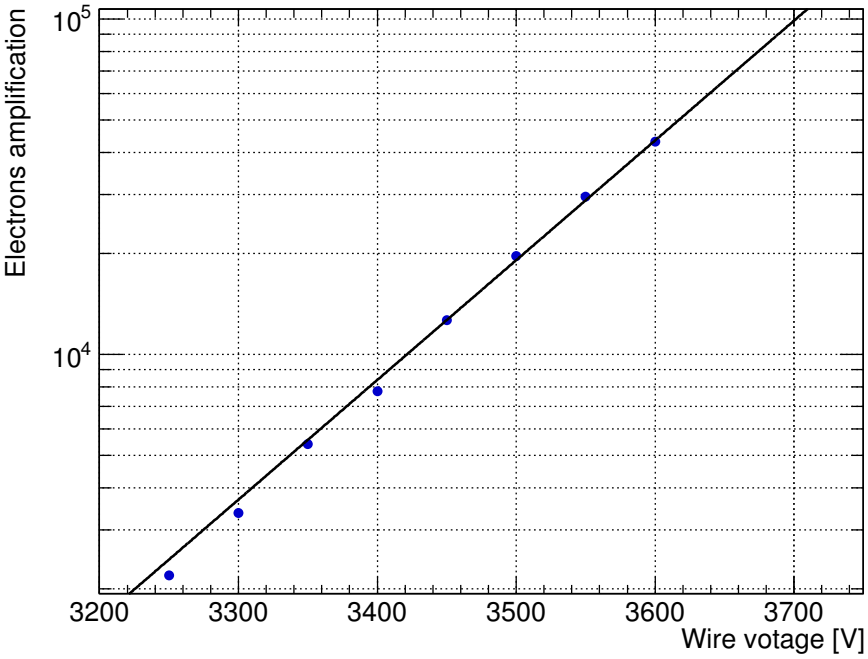

Figure 20: Amplification near the wire as a function of wire voltage

7 Acknowledgements

The work has been done at the LNL laboratories of INFN. The report is a summary of the activity performed during the stage of the first year of the master in physics by the student G. Mocellin, in collaboration with Doct. F. Gonella, Prof. F. Gasparini and Prof. A. T. Meneguzzo. The authors want to thanks Ing. Mimmo Dattola (INFN of Torino) for the drawings and the help on the constructions of the bicells; S. Carturan and V. Maggioni and all the LNL for the support.

References

[1] **DT Gif++ meeting 18-Aug-2016**, D.Dattola, D.Fasanella, F.Gasparini, F.Gonella, A.T.Meneguzzo, J.Pazzini, I.Redondo, *"GIF++ STUDIES"*.

[2] **International workshop on Aging Phenomena in Gaseous Detectors, 2-5/10/2001, DESY, Hamburg**, M. Capeans, *"Materials and gases: Lessons for detectors and gas systems"*.

[3] **ECFA High Luminosity LHC Experiments Workshop, 22/10/2014**, G. Graziani, *"Wire detectors @ HL-LHC"*.

[4] **JINST 5 (2010) T03016 CMS-CFT-09-023**, The CMS Collaboration, *"Calibration of the CMS Drift Tube Chambers and Measurement of the Drift Velocity with Cosmic Rays"*.

[5] **JINST 5 (2010) T03015 arXiv:0911.4855 [physics.ins-det] CMS-CFT-09-012 CMS Paper CFT-09-012**, The CMS Collaboration, *"Performance of the CMS Drift Tube Chambers with Cosmic Rays"*.

[6] **JINST 8 (2013) P11002 DOI: 10.1088/1748-0221/8/11/P11002**, The CMS Collaboration, *"The performance of the CMS muon detector in proton-proton collisions at $\sqrt{s} = 7$ TeV at the LHC"*.

[7] **Nucl. Instrum. and Meth. A 579 (2007), 951-960, DOI: 10.1016**, M. Aldaya et al. *"Results of the first integration test of the CMS drift tubes muon trigger"*.

[8] **Nucl.Instrum.Meth. A480 (2002) 658-669, 12 pp**, M. Aguilar-Benitez et al., *" Construction and test of the final CMS Barrel Drift Tube Muon Chamber prototype"*.

[9] **LHC electronics workshop,2001**, F. Gonella and M. Pegoraro, *"The MAD", a Full Custom ASIC for the CMS Barrel Muon Chambers Front End Electronics"*.

[10] **JINST 5 (2010) T03003 CMS-CFT-09-022 DOI: 10.1088/1748-0221/5/03/T03003**, The CMS Collaboration, *"Performance of the CMS Drift Tube Local Trigger with Cosmic Rays"*.

[11] **CERN-PH-EP/2012-173 2013/03/21**, The CMS Collaboration, *"Performance of CMS muon reconstruction in pp collision events at $\sqrt{s} = 7$ TeV"*.

[12] **CMS NOTE 2007/000**, M. Benettoni, F. Gasparini, F. Gonella, A. Meneguzzo, S. Vanini, G. Zumerle, G. Bonomi, *"CMS DT Chambers: Optimized Measurement of Cosmic Rays Crossing Time in absence of Magnetic Field"*.

[13] **http://www.spectrumtechniques.com/radioisotopes2.htm**

[14] **Lectures given in the Academic Training Programme of CERN 1975-1976, CERN-77-09**, F. Sauli, *"Principles of operation of multiwire proportional and drift chambers"*.

[15] **Chin. Phys. C, 2015**, Particle Data Group, *"The Review of Particle Physics"*.